UC Davis
UC Davis Previously Published Works

Title

A pair of receptor-like kinases is responsible for natural variation in shoot growth response to mannitol treatment in Arabidopsis thaliana

Permalink

https://escholarship.org/uc/item/7fh873q3

Journal

The Plant Journal, 78(1)

ISSN

0960-7412

Authors

Trontin, Charlotte
Kiani, Seifollah
Corwin, Jason A
et al.

Publication Date

2014-04-01

DOI

10.1111/tpj.12454

Peer reviewed

A pair of receptor-like kinases is responsible for natural variation in shoot growth response to mannitol treatment in *Arabidopsis thaliana*

Charlotte Trontin[1,2], Seifollah Kiani[1,2], Jason A. Corwin[3], Kian Hématy[1,2], Jennifer Yansouni[4], Dan J. Kliebenstein[3] and Olivier Loudet[1,2,*]

[1]INRA, UMR1318, Institut Jean-Pierre Bourgin, RD10, F-78000 Versailles, France,
[2]AgroParisTech, Institut Jean-Pierre Bourgin, RD10, F-78000 Versailles, France,
[3]Department of Plant Sciences, University of California-Davis, Davis, CA 95616, USA, and
[4]Unité de Recherche en Génomique Végétale, Plateforme Transcriptome, UMR1165, INRA, Université d'Evry Val d'Essonne, 2 rue G. Crémieux, F-91057 Evry, France

SUMMARY

Growth is a complex trait that adapts to the prevailing conditions by integrating many internal and external signals. Understanding the molecular origin of this variation remains a challenging issue. In this study, natural variation of shoot growth under mannitol-induced stress was analyzed by standard quantitative trait locus mapping methods in a recombinant inbred line population derived from a cross between the Col-0 and Cvi-0 *Arabidopsis thaliana* accessions. Cloning of a major QTL specific to mannitol-induced stress condition led to identification of *EGM1* and *EGM2*, a pair of tandem-duplicated genes encoding receptor-like kinases that are potentially involved in signaling of mannitol-associated stress responses. Using various genetic approaches, we identified two non-synonymous mutations in the *EGM2*[Cvi] allele that are shared by at least ten accessions from various origins and are probably responsible for a specific tolerance to mannitol. We have shown that the enhanced shoot growth phenotype contributed by the Cvi allele is not linked to generic osmotic properties but instead to a specific chemical property of mannitol itself. This result raises the question of the function of such a gene in *A. thaliana*, a species that does not synthesize mannitol. Our findings suggest that the receptor-like kinases encoded by *EGM* genes may be activated by mannitol produced by pathogens such as fungi, and may contribute to plant defense responses whenever mannitol is present.

Keywords: *Arabidopsis thaliana*, natural variation, pathogen, mannitol, QTL, receptor-like kinase.

INTRODUCTION

Despite being physiologically disputable (Verslues *et al.*, 2006), mannitol-treated plants are still widely used as a means to induce responses *in vitro*, including as a substitution for drought stress assays, as they mimic osmotic constraints. The exogenous application of mannitol has helped to reveal transcriptomic pathways that are at least partially relevant to abiotic stress responses in general, and also to biotic interactions (Skirycz *et al.*, 2010). It remains unclear whether mannitol treatment highlights cross-talk between stresses induced by the general chemical properties of mannitol (especially its osmotic properties) or by structurally specific features of mannitol (Chan *et al.*, 2011). Mannitol, the chemically reduced form of mannose, is a compatible solute that is accumulated by several plant species as a

carbon storage and translocation form, and in response to abiotic stresses (Stoop *et al.*, 1996). Despite harboring some mannitol transport and enzymatic components, *Arabidopsis thaliana* is not known to accumulate mannitol, and mannitol is not recognized as playing any obvious specific role in this species (Stoop *et al.*, 1996; Klepek *et al.*, 2005; Reinders *et al.*, 2005). In addition to endogenous sources, plants are exposed to external sources of mannitol in nature, specifically from numerous fungal pathogens that produce significant amounts of mannitol during the infection process (Velez *et al.*, 2008). Recent work has shown that other specific sugars, previously thought to function solely as osmoticums, have structure-dependent regulatory capacities (Wahl *et al.*, 2013).

To study the mechanistic basis of how plants respond to mannitol, we exploited the natural variation of mannitol responses in *A. thaliana*. Natural variation and quantitative genetics approaches represent functionally non-*a priori* strategies to reveal new genes or alleles involved in the variation of complex traits (Trontin *et al.*, 2011). However, the QTL mapping outcome is directly conditioned by the variation segregating in the genetic material used, especially in a specific cross. The main sources of variation uncovered may only be very indirectly related to the initially intended screen (Masle *et al.*, 2005; Poormohammad Kiani *et al.*, 2012). In this study, we made use of existing recombinant inbred lines (RILs) set between the genetically distant accessions Cvi-0 and Col-0 to map and clone a major effector of the plant response to mannitol. This corresponds to variation in at least one of two putative receptor-like kinases (RLKs) duplicated in tandem that are directly involved in the plant-specific response to mannitol itself (not its osmotic effect) and in activating several pathogen defense components. We describe a pathogen-tolerance phenotype associated with variation in this step.

RESULTS

Mapping of the EGM QTL

Natural variation for seedling growth under both control and mannitol-supplemented conditions was investigated in a core set of 164 RILs issued from the Cvi-0 × Col-0 cross, by estimating seedling area *in vitro* at a young stage. Along with other smaller-effect QTLs, a major locus that controlled growth under mannitol was mapped to the top of chromosome 1, and explains approximately 37% of the total phenotypic variance, with a positive allelic contribution from the Cvi allele (Figure S1A). A 2D scan of the genome revealed no epistatic interaction with any other locus. The segregation of this QTL, named EGM (for enhanced shoot growth under mannitol stress), was confirmed by using a heterogeneous inbred family (HIF170). Direct phenotyping of the progeny of the heterozygous RIL170 (progeny testing), as well as phenotyping of the fixed homozygous lines HIF170[Col] and HIF170[Cvi], confirmed specific segregation of the QTL under mannitol stress conditions, and revealed that the Col allele is almost completely dominant over the Cvi allele (Figure S1B). To identify the gene underlying the EGM QTL, fine-mapping was performed using a series of recombinants (rHIFs) derived from HIF170, and ultimately reduced the candidate interval to 10 kb (Figure S1C). Analysis of advanced recombined HIFs (arHIFs, obtained after crossing the two most informative rHIFs) segregating solely for the 10 kb interval (Figure 1a and Figure S1D) confirmed that the 3790–3800 kb interval of chromosome 1 is sufficient to cause the EGM-associated phenotype.

The 10 kb candidate region contained three predicted open reading frames according to the Arabidopsis Information Resource (http://www.arabidopsis.org/): *At1g11280*, encoding a putative RLK, *At1g11290*, encoding a Pentatricopeptide Repeat Protein endonuclease, and *At1g11300*, which was annotated as a double RLK containing the same structural unit duplicated in tandem. Such a double structure is quite uncommon for a kinase (Shiu and Bleecker, 2001b), and was indeed predicted to comprise two open reading frames by the GeneFarm algorithm (http://urgi.versailles.inra.fr/Genefarm/) (Figure 1b). To clarify the number of open reading frames encoded in the region encompassing *At1g11300*, we performed RT-PCR on the total RNA of the arHIFs. It was possible to amplify each structural unit independently in both arHIFs, but amplification of a fragment encompassing both of them was not possible, suggesting that the two structural units are transcribed independently. These results were confirmed by 3′ RACE, which allowed detection of unique polyA tails at the end of the first and second structural units. To summarize, four open reading frames are present in the candidate interval: *At1g11280*, *At1 g11290*, *At1 g11300* and *At1g11305* (Figure 1b).

Two polymorphisms that are probably responsible for *At1g11305* hypo-functionality contribute to the EGM QTL

To identify the EGM causative gene, several T-DNA insertion mutants in the four candidate genes were analyzed (Figure 1b). Four T-DNA insertion lines in the coding sequence of *At1 g11300* or *At1 g11305* and one insertion line in the promoter of *At1 g11300* (affecting transcript accumulation; Figure S2C) all showed significantly better growth on medium supplemented with 60 mM mannitol (Man60) than homozygous WT (wild-type) lines, and a significant genotype × medium interaction (SALK_058300, WISC_DsLox426E06, SAIL_150_H02 and SALK_008433) or a much more significant effect under Man60 conditions (SALK_044069) (Figure 1c and Figure S2A). In addition, we generated an amiRNA line that specifically targeted both the *At1 g11300* and *At1 g11305* transcripts, which also showed a significant mannitol-dependent growth phenotype (Figure S2B,C). This phenotype was not observed among T-DNA insertion lines for other genes of the candidate region. This suggests that the putative RLKs encoded by *At1 g11300* and *At1 g11305*, which are important for the plant growth response to mannitol, are good candidates for the EGM QTL.

We named the first gene *EGM1* (*At1 g11300*) and the second one *EGM2* (*At1 g11305*). They encode two closely related proteins (86.7% identity) from the SD1 RLK family (Lehti-Shiu *et al.*, 2009). RLKs are characterized by the presence of a signal sequence, a ligand-binding extracellular domain, a transmembrane region and an intracellular C-terminal kinase domain, all of which are present in the full-length predicted EGM proteins (Figure 1d). The SD1 sub-family is characterized by a B-lectin domain (Curculin-
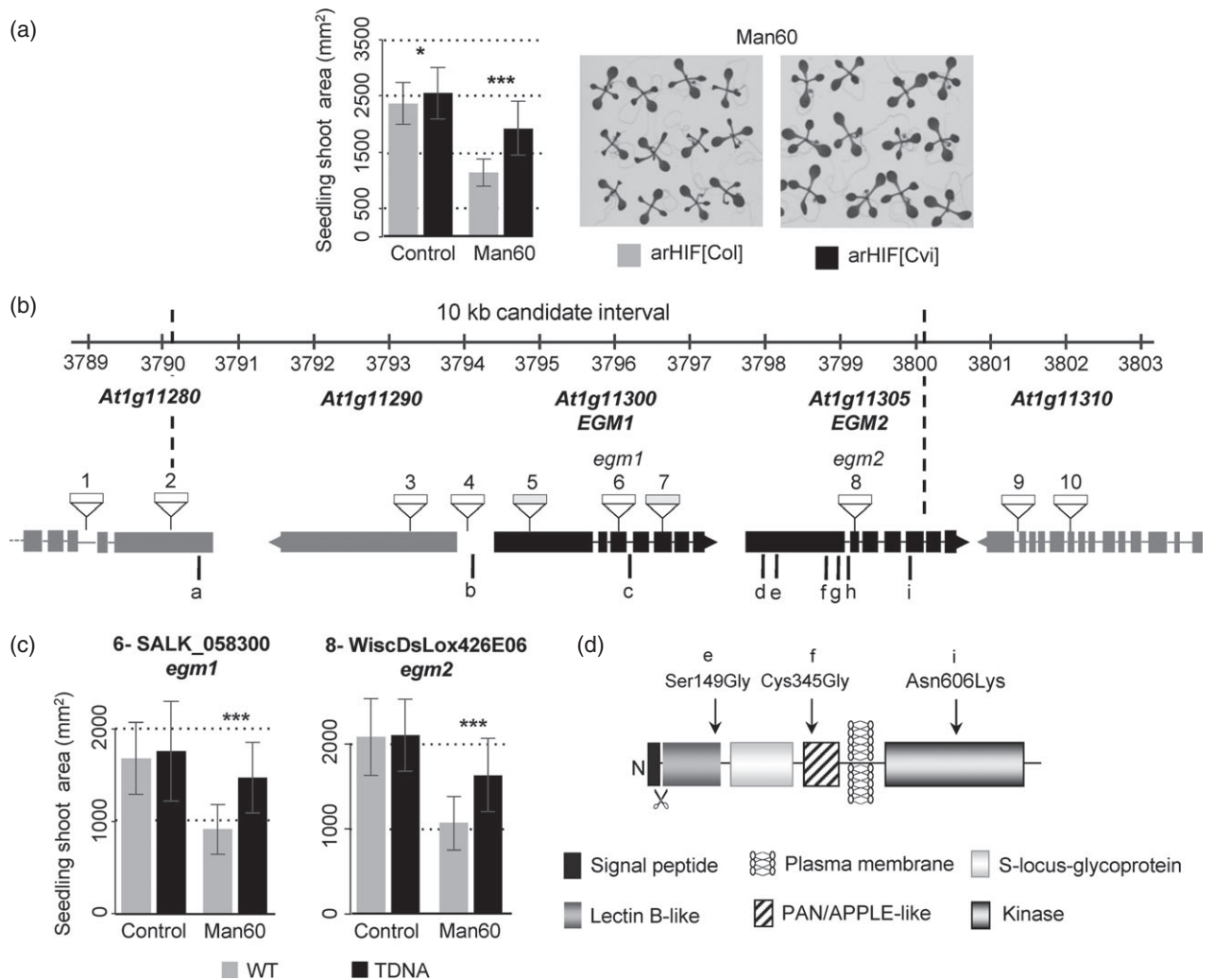
Figure 1. Two genes in a 10 kb interval are strong candidates for the EGM QTL.

(a) Phenotyping of arHIF[Col] and arHIF[Cvi] at 12 DAS under control conditions and on medium supplemented with 60 mM mannitol (Man60) confirmed the segregation of the EGM QTL in a 10 kb interval. The images on the right illustrate the phenotype of the arHIFs on Man60.

(b) The 10 kb candidate interval on chromosome 1 confirmed by the arHIF is indicated by dashed vertical lines. Physical positions are indicated in kb. Gene models predicted using the GeneFarm algorithm (http://urgi.versailles.inra.fr/Genefarm/) (arrows) are represented (filled rectangles correspond to exons), except for *At1g11310* (TAIR version 10 gene prediction). The approximate insertion sites of T-DNA are indicated: (1) SALK_206891, (2) WiscDsLoxHs015_10B, (3) SALK_122320, (4) SALK_008433, (5) SAIL_150_H02, (6) SALK_058300, (7) SALK_044069, (8) WiscDsLox426E06, (9) SALK_050191, (10) SALK_07985. SNPs observed between Col and Cvi alleles are indicated by the letters 'a'–'i'. For the nature of the mutations, see Figures 1(d) and 2.

(c) Phenotyping of *egm1* and *egm2* T-DNA mutants on control and Man60 media.

(d) Model of the protein structure of EGM1 and EGM2 RLKs. The peptide signals (amino acids 1–27) and transmembrane region (amino acids 439–461) were predicted using the SignalP 3.0 server (http://www.cbs.dtu.dk/services/SignalP-3.0/) and the TMHMM server version 2 (http://www.cbs.dtu.dk/services/TMHMM/), respectively. Non-synonymous mutations identified in *EGM2* between the Col and Cvi allele are indicated.

Error bars represent SD obtained from the phenotyping of at least 30 plants, and a second biological replicate gave similar results. Asterisks indicate significant genotypic effects for each medium (*$0.01 < P < 0.05$, ***$P < 0.001$, Student's t test).

like domain/agglutinin motif) that is predicted to be involved in mannose binding (Ramachandraiah and Chandra, 2000; Shiu and Bleecker, 2001a; Wasano *et al.*, 2003), an S-locus glycoprotein domain, and a PAN/APPLE-like domain that is expected to be involved in protein/protein or carbohydrate/protein interactions (Tordai *et al.*, 1999; Shiu and Bleecker, 2001a). Phylogenetic analysis of the SD1 sub-family revealed that *EGM1* and *EGM2* are close paralogs that resulted from a tandem gene
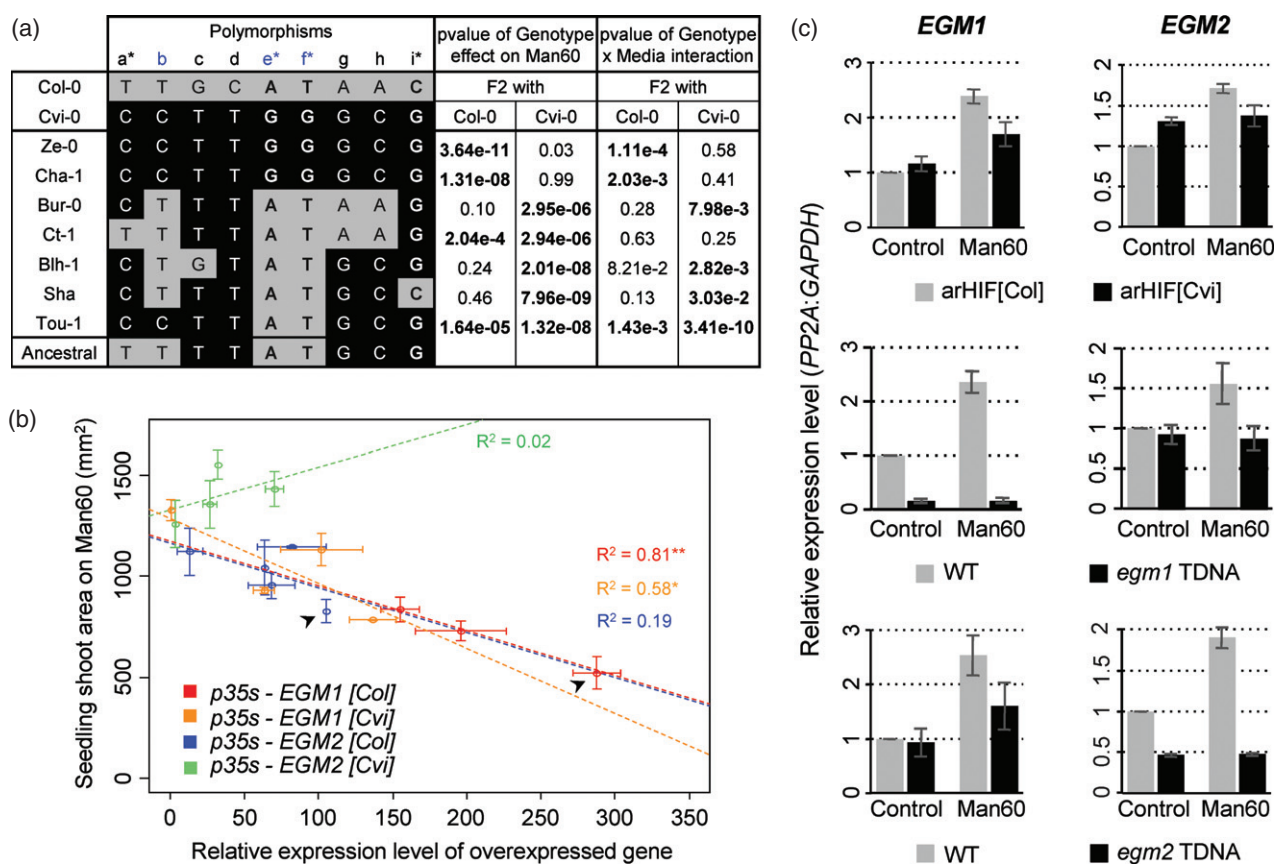
duplication probably around the time of divergence from *Arabidopsis lyrata*, in which only a clear *EGM1* ortholog is identified (Figure S3A).

Within the 10 kb candidate region, nine polymorphisms were identified between Col-0 and Cvi-0 ('a'–'i'). Six of the nine were located in *EGM2* (including three non-synonymous polymorphisms: 'e' = S149G, 'f' = C345G, 'i' = N606K) versus two polymorphisms in non-coding regions of *EGM1* (Figures 1b,d and 2a). To identify which

of these polymorphisms were causal for the QTL, i.e. to identify the quantitative trait nucleotide(s), we tested EGM phenotypic segregation in several crosses (F_2 progeny) designed to segregate for diverse combinations of Col and Cvi polymorphisms at positions 'a' to 'i', an approach that we named 'specific association genetics'. This approach is not necessarily uncompromised, as we cannot totally exclude the possibility that the patterns of observed phenotypic segregation may be explained by other linked polymorphisms (including those in Table S1) or influenced by other QTLs segregating specifically in each F_2 population. To avoid genetic and environmental bias and possible maternal effects, we performed this approach using several independent accessions whenever possible, in independent experiments and/or on reciprocal crosses to Col-0 and Cvi-0. First, we tested this approach on two accessions of 13 presenting the same haplotype as Cvi-0 at

polymorphisms 'a' to 'i' (Figure 2a). These were redundant to Cvi-0 when crossed with Col-0 in terms of segregation of EGM, validating this approach and confirming that EGM may be associated with at least one of the polymorphisms segregating in the 10 kb interval. Four other accessions bearing a mix of Col and Cvi polymorphisms at positions 'a'–'i' (Bur-0, Ct-1, Shahdara and Blh-1) essentially segregate in crosses with Cvi-0 but not Col-0, restricting the list of candidate quantitative trait nucleotides to three (polymorphisms 'b', 'e' and 'f'; Figure 2a).

Polymorphisms 'e' and 'f' result in important amino acid changes in the Cvi version of EGM2. The first change was mutation of a serine (conserved throughout the SD1 family) into a glycine in the lectin domain of the SD1 receptor. The second change involved a highly conserved cysteine that may be one of the conserved cysteines of the PAN/APPLE-like domain that is involved in disulfide bonds and

	Polymorphisms									pvalue of Genotype effect on Man60		pvalue of Genotype x Media interaction	
	a*	b	c	d	e*	f*	g	h	i*				
										F2 with		F2 with	
Col-0	T	T	G	C	A	T	A	A	C	Col-0	Cvi-0	Col-0	Cvi-0
Cvi-0	C	C	T	T	G	G	G	C	G				
Ze-0	C	C	T	T	G	G	G	C	G	3.64e-11	0.03	1.11e-4	0.58
Cha-1	C	C	T	T	G	G	G	C	G	1.31e-08	0.99	2.03e-3	0.41
Bur-0	C	T	T	T	A	T	A	A	G	0.10	2.95e-06	0.28	7.98e-3
Ct-1	T	T	T	T	A	T	A	A	G	2.04e-4	2.94e-06	0.63	0.25
Blh-1	C	T	G	T	A	T	G	C	G	0.24	2.01e-08	8.21e-2	2.82e-3
Sha	C	T	T	T	A	T	G	C	C	0.46	7.96e-09	0.13	3.03e-2
Tou-1	C	C	T	T	A	T	G	C	G	1.64e-05	1.32e-08	1.43e-3	3.41e-10
Ancestral	T	T	T	T	A	T	G	C	G				

Figure 2. Two polymorphisms in *EGM2* are probably responsible for the EGM QTL.
(a) Specific association genetics identified three polymorphisms ('b', 'e' and 'f') as candidates for the QTL. The SNPs identified between the Col and Cvi alleles ('a'–'i', Figure 1b) are indicated, as well as their state in seven additional accessions. The 'ancestral' haplotype corresponds to that retrieved from *A. lyrata* *EGM1* (A.ly #910885 sequence). Asterisks indicate non-synonymous polymorphisms (Figure 1d). The segregation of EGM in F_2 progeny from crosses to Col-0 or Cvi-0 was tested by ANOVA.
(b) Transgenic complementation of arHIF[Cvi] with the Col and Cvi alleles of *EGM1* and *EGM2* under the control of the CaMV 35S promoter. Arrowheads indicate the lines that were further analyzed for mannitol stress-responsive genes (Figure S6D). Asterisks indicate the significance of the effect of the relative expression level of the over-expressed gene on the phenotype on Man60 (*$P < 0.05$, **$P < 0.01$; ANOVA). Adjusted R^2 values are also indicated.
(c) Relative expression levels of *EGM1* and *EGM2* in the arHIFs and the *egm1* (SALK_058300) and *egm2* (WiscDsLox426E06) mutants.
Expression levels were normalized with respect to the expression level of *EGM1* or *EGM2* in arHIF[Col] on Man60 (b), or in arHIF[Col] or WT under control conditions (c). Error bars represent the SD observed among two biological replicates from two independent experiments.

is important for the conformation of the domain (McMullen *et al.*, 1991) (Figure 1b,d). Therefore, these mutations are likely to affect EGM2 functionality and one of them, or both, may explain the QTL. To confirm this hypothesis, we complemented arHIF[Cvi] with the Col and Cvi allele of either *EGM1* and *EGM2* under the control of the CaMV 35S promoter. Interestingly, expression of all the transgenes except *EGM2*[Cvi] complemented the phenotype in the arHIF[Cvi] background; in addition, seedling size on Man60 was clearly negatively correlated with the *EGM1* expression level, whose over-expression was stronger than that of *EGM2* (Figure 2b). *EGM2*[Cvi] did not affect growth of *A. thaliana* in the presence of mannitol, and thus is probably hypo-functional compared to *EGM2*[Col], probably due to the S149G and C345G mutations. The results of this experiment show that the level of expression of the *EGM* genes is important for shoot growth limitation in response to mannitol.

On the basis of this result and to test whether polymorphism 'b' in the promoter of *EGM1* also contributes to the EGM phenotype, we analyzed the level of expression of both genes using specific TaqMan probes under control and Man60 conditions in the arHIFs. Both genes were induced under mannitol stress in arHIF[Col]. However, in arHIF[Cvi], the induction of *EGM1* was reduced and no induction of *EGM2* was observed (Figure 2c). Interestingly, expression analysis in *egm1* and *egm2* mutants revealed that induction of *EGM1* was at least partially dependent on the functionality of EGM2, and that induction of *EGM2* was completely dependent on EGM1 functionality. The reduction of the induction of *EGM1* observed in arHIF[Cvi] may therefore be explained by the EGM2[Cvi] hypo-functionality. Nevertheless, we cannot totally exclude the possibility that polymorphism 'b' in the promoter of *EGM1* may also contribute to this reduction of expression as the expression level of both genes in accession Tou-1 (Col-like for polymorphisms 'e' and 'f' and Cvi-like for polymorphism 'b') is more similar to that of Cvi-0 than Col-0 (Figure S4). Indeed, the Tou allele at the EGM QTL presented an intermediate state between the Col and Cvi alleles when tested in F_2 progeny (Figure 2a). As we only found and analyzed one such accession (Tou-1), these results may also be explained by additional specific polymorphisms in Tou-1.

Taken as a whole, our results strongly suggest that at least one of two non-synonymous polymorphisms in *EGM2* is responsible for the QTL, and that both EGM1 and EGM2 control plant growth responses to mannitol.

EGM1 and EGM2 act together in the mannitol stress response

Although phylogenetically close, single mutants of both *EGM1* and *EGM2* show enhanced shoot growth under mannitol treatment, suggesting that they are not fully redundant

(Figure 1c). Conversely, a p35s:*EGM1* construct was able to complement arHIF[Cvi], which carries an hypo-functional allele of *EGM2* (Figure 2b), suggesting that the two genes may be functionally equivalent. To check whether *EGM1* may substitute for *EGM2* even when expressed at endogenous expression levels, we compared complementation of the *egm2* mutant with *EGM1* and *EGM2* genes under the control of their endogenous promoters (approximately 1 kb upstream of the ATG codon). Whereas the *pEGM2:EGM2* construct phenotypically complemented the *egm2* mutant in the four insertion lines analyzed (Figure 3a), *pEGM1: EGM1* only complemented *egm2* in one of four lines (line A, Figure 3a), but fully complemented the *egm1* mutant. Transcript accumulation analyses revealed that the level of expression of *EGM1* in *egm2 pEGM1:EGM1* insertion lines B, C and D was equivalent or higher than that of *EGM2* in the *egm2 pEGM2:EGM2* lines, thus the complementation difference between the two constructs is not simply explained by a difference in their expression level, while the phenotype of insertion line A may be explained by a higher level of transcript accumulation (Figure 3a). The data suggests that *EGM1* complements *egm2* only when expressed at a very high level, and that these two paralogs are not fully redundant in Col-0.

Finally, complementation of the *egm2* mutant with the 8 kb region encompassing the 1 kb promoter of *EGM1* towards the end of *EGM2* led to an increase of the level of expression of the two genes and stronger growth reduction on Man60, suggesting that the two RLKs act together to induce an EGM response and are limiting for this pathway leading to growth reduction. Phenotyping of two independent lines (Col-0 background) transformed with an amiRNA construct targeting both genes also suggested that EGM1 and EGM2 are involved in the same pathway (Figure S2B). The more thoroughly defined *EGM1* promoter was used in a fusion with a GUS reporter and transformed into Col-0. Almost no GUS staining was detected in 15-day-old seedlings grown under control conditions, but a signal was observed in the shoot meristem and young leaves of seedlings grown under Man60 condition in five of seven insertion lines (Figure 3b). This expression pattern suggests that the gene acts during early leaf development to induce growth inhibition under mannitol treatment. Thus, it may be concluded that EGM1 and EGM2 both function to reduce growth under mannitol treatment but are not fully redundant.

To determine whether other members of the SD1 subfamily are involved in the mannitol response, we analyzed T-DNA mutants in several SD1 members that were closely related to *EGM1*/*EGM2* and/or up-regulated by mannitol treatment according to Kilian *et al.* (2007). Among the seven genes we tested, we found no obvious phenotypic indication for their involvement in the mannitol response (Figures S2A and S3B).
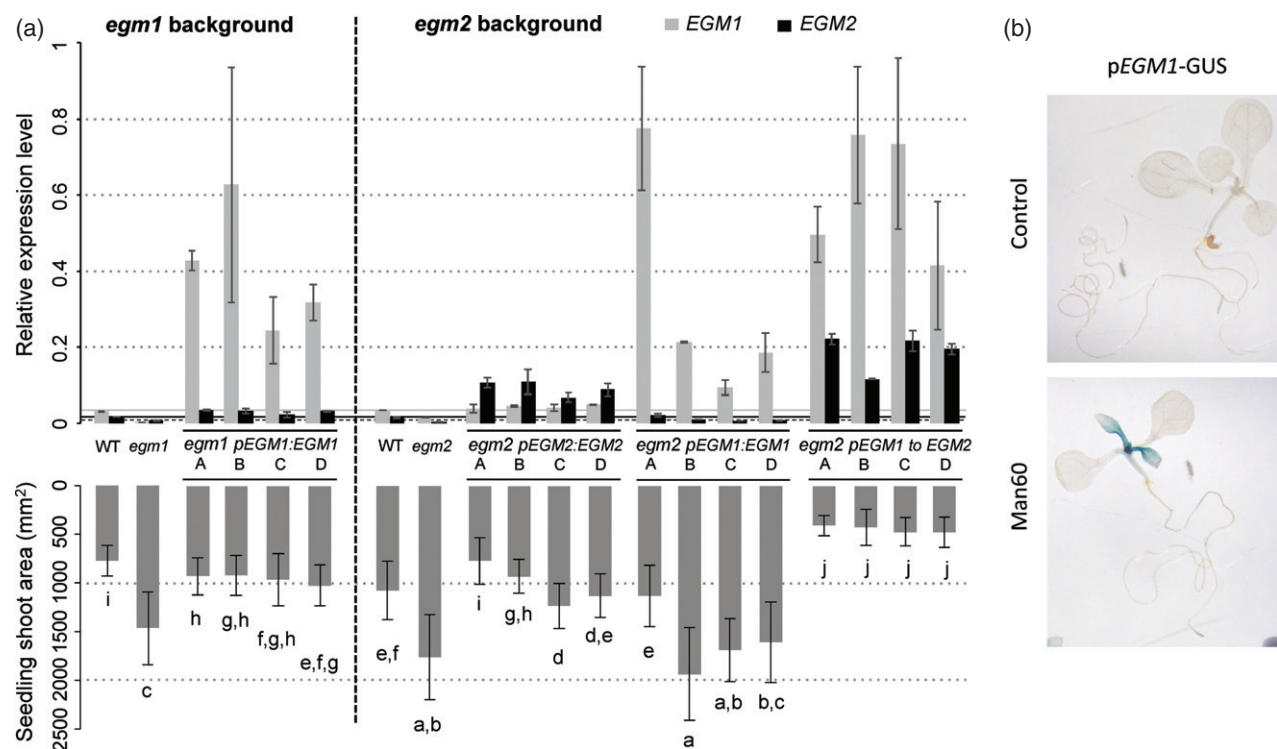
Figure 3. EGM1 and EGM2 are not fully redundant regarding mannitol stress response.
(a) Complementation of *egm1* and *egm2* mutants with *EGM1* or *EGM2* genes under the control of their endogenous promoters (1 kb upstream of the ATG codon) or with the region covering the 1 kb promoter of *EGM1* towards the end of *EGM2* (approximately 8 kb). The shoot area and the expression of *EGM1* and *EGM2* were measured on 12 DAS seedlings grown on Man60. Different letters indicate significantly different results based on a *post hoc* Kruskal–Wallis test ($P < 0.05$). Error bars represent the SD observed in two biological replicates from two independent experiments (expression level) or the SD obtained from phenotyping of at least 30 plants (seedling shoot area). For phenotyping data, a second biological replicate gave similar results.
(b) Histochemical analysis of GUS reporter gene expression driven by the *EGM1* promoter (1 kb upstream of the ATG codon) in whole 12 DAS seedlings grown under control conditions or on Man60 medium.

Toward EGM function

In this paper, mannitol was used in the *in vitro* medium to induce a response. As EGM2 contains both putative mannose-binding and putative carbohydrate-binding domains, we wished to determine whether the variation in shoot growth results from the osmotic stress imposed by mannitol or an action specific to mannitol.

To answer this question, we tested the segregation of EGM under various osmotic constraints, such as those generated using NaCl, KCl, mannose and sorbitol-supplemented media. NaCl and KCl induce general osmotic stresses via ionic perturbation of the plant, while mannose, mannitol and sorbitol alter the osmotic status due to non-ionic solute changes; these treatments have been shown to induce distinct responses *in planta* (e.g. Kreps *et al.*, 2002; Parre *et al.*, 2007). If there is overlap in the behavior of the EGM alleles across these stresses, then the response must be due to osmotic effects; however, if the growth response is unique to mannitol then the genetic interaction of mannitol with EGM is specific. None of these other conditions resulted in any consistently significant growth phenotype for the different deficient EGM alleles (Cvi or

T-DNA insertion alleles; Figure 4a and Figure S5A). The segregation of the QTL in the arHIF background was also tested under drought stress on soil plugs at later stages of development, but no significant genotypic effect or genotype × drought interaction was observed (Figure 4b). Interestingly, the growth difference observed between the arHIFs is established at relatively moderate mannitol concentrations (≤ 10 mM) and is maintained at higher mannitol concentrations, while the shoot size continues to decrease, probably due to the osmotic stress component (Figure S5B). These results suggest that the growth response mediated by EGM1 and EGM2 is specific to mannitol treatment and is not a consequence of general osmotic constraint perception. This raises the question of why *A. thaliana*, which does not naturally synthesize mannitol, expresses EGM1 and EGM2 RLKs that mediate a specific growth response to mannitol.

To understand the link between these proteins and the mannitol response, the transcriptomes of arHIF[Col] and arHIF[Cvi] on Man60 medium were compared using CATMA microarrays. A total of 221 genes were differentially expressed between the two arHIFs, most of which (199) were up-regulated in arHIF[Col] compared to arHIF
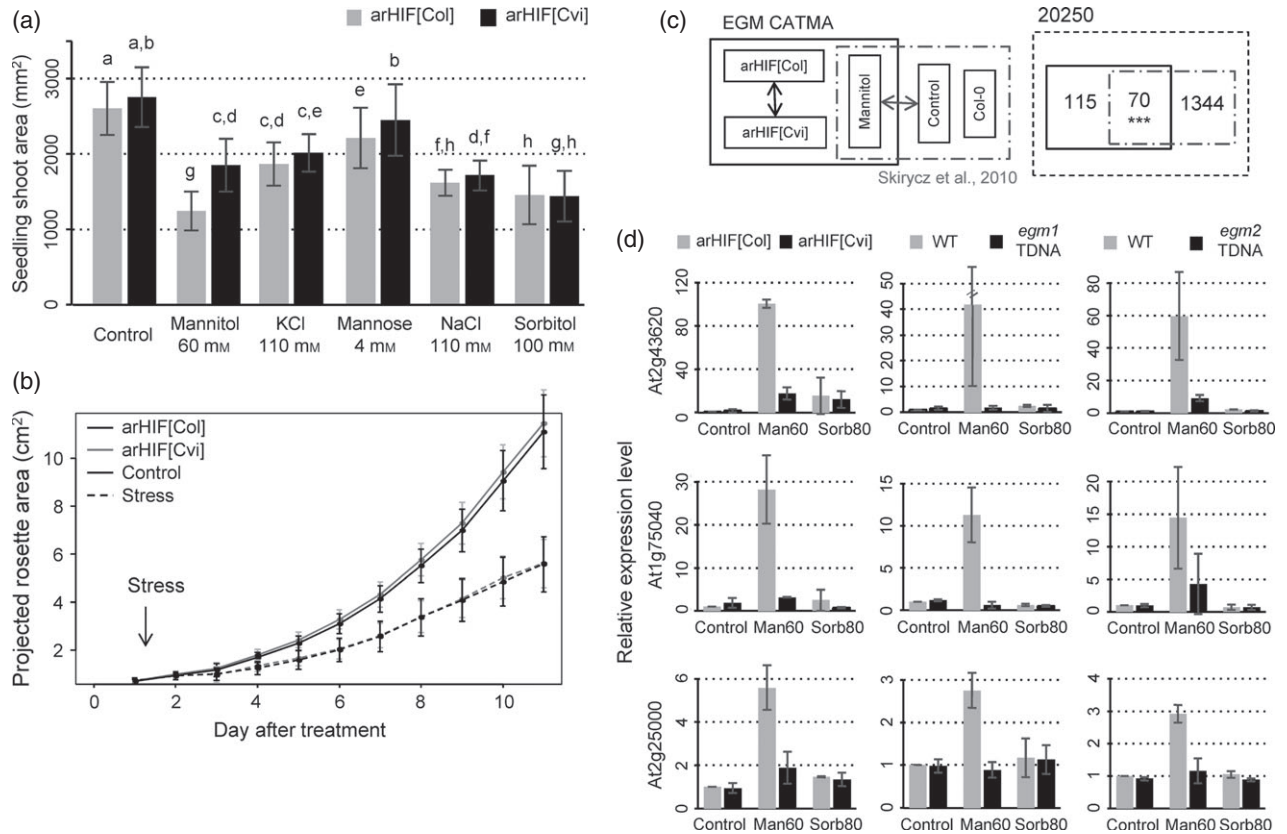
Figure 4. The enhanced shoot growth phenotype observed in *egm1* and *egm2* mutants on Man60 is probably not the result of an osmotic constraint.
(a) Phenotyping of 12 DAS seedlings of arHIF[Col] and arHIF[Cvi] grown under various osmotic constraints. Different letters indicate significantly different results based on a *post hoc* Tukey's honest significant difference test ($P < 0.05$). A second biological replicate gave similar results.
(b) Phenotyping of arHIF[Col] and arHIF[Cvi] on soil plugs under control conditions (60% of plug soil water content) or drought stress conditions (30% of plug soil water content) for 10 days. At day '0' on the figure, the plants were already 14 days old. Error in (a) and (b) bars represent the SD obtained from the phenotyping of at least 30 plants.
(c) Comparison of the set of genes differentially expressed between the two arHIFs on Man60 medium (EGM CATMA) with the set of genes previously identified (Skirycz *et al.*, 2010) as differentially expressed in expanding cells of the Col-0 accession grown under control conditions or on medium supplemented with 25 mM mannitol. The overlap between the two sets, which comprises genes that were differentially expressed in the same direction in the two analyses, was tested using the Genesect tool available on the Virtual Plant 1.3 website. The 20 250 TAIR version 10 gene models that are common between the CATMA version 5 arrays and Affymetrix ATH1 arrays were used as the background list.
(d) Relative transcript accumulation of three genes shared between our transcriptomic analysis and that by Skirycz *et al.* (2010) in 12 DAS seedlings of the arHIFs and the *egm1* and *egm2* mutants grown under control conditions, or on medium supplemented with 60 mM mannitol or 80 mM sorbitol (Man60 and Sorb80, respectively). At2g43620, chitinase; At1g75040, *PR5*; At2g25000, *WRKY60*. Error bars represent the SD obtained from two biological replicates from two independent experiments.

[Cvi] (Table S2). Biological GO analysis of this set of genes revealed a significant enrichment in genes involved in responses to stimuli, including genes responding to abiotic and biotic stimuli (Figure S6A). Comparison of our transcriptomic analysis with previous work studying the response of Col-0 seedlings to treatment with 25 mM mannitol showed a significant overlap ($P < 0.001$, non-parametric randomization test): 185 of the 221 genes differentially expressed between the arHIFs were also interrogated by Skirycz *et al.* (2010), of which 70 were also found to be mannitol-responsive genes (Figure 4c). These observations were validated by quantitative PCR on seven of the nine genes that we tested among the 70 (Figure 4d and Figure S6B), including three genes typically found in the GO class for the biotic stress response

(such as *PR5*) and two chitinases. These genes were induced specifically or at a much higher level on Man60 (and not on medium supplemented with 80 mM sorbitol) in arHIF[Col] compared with arHIF[Cvi]. We further confirmed that this induction was dependent on both EGM1 and EGM2 functionality in the mutants and amiRNA lines for three genes (Figure 4d and Figure S6C). The results at the transcriptomic level mirrored the growth phenotypes, and suggested that the defective EGM genotypes (arHIF [Cvi] and *egm* mutants) behave like plants that do not perceive and respond to mannitol. Additionally, in the over-expressors, the transcriptomic response was opposite to that in the defective genotypes, consistent with a stronger phenotypic response in the two analyzed lines (Figure S6D).

The specificity of the mannitol response in contrast to other osmotic stresses at both the phenotypic and transcriptomic level, combined with the enrichment in genes belonging to the biotic stress GO category in our CATMA analysis, suggested that EGM may be involved in the biotic stress response. It is known that some pathogens, including fungi, use mannitol for carbon storage, and it has been suggested that mannitol may be secreted by pathogens during infection to counteract plant production of reactive oxygen species (ROS), and that the plant may react against this phenomenon (Jennings *et al.*, 1998). To test the role of EGM1 and EGM2 in plant defense against pathogens, we evaluated the sensitivity of the *egm* mutants to *Botrytis cinerea* using two isolates (BcGrape and Bc83-2). Both the *egm1* and *egm2* mutants were more susceptible to the two *Botrytis* isolates than Col-0, as shown by the larger perimeter of the necrotic region 72 h post-infection (Figure 5a). Similar results were found with the arHIFs despite the higher intrinsic sensitivity of this genetic background (Figure S7A). A significant interaction between plant genotype and *Botrytis* isolates was observed (ANOVA, $P < 0.001$), with a stronger response to the BcGrape isolate, which produced significantly larger amounts of mannitol within the plant lesion (Kruskal–Wallis test, $P < 0.001$; Figure 5b and Figure S7B). Thus, both EGM1 and EGM2 contribute to pathogen defenses that correlates with the level of mannitol secreted by the pathogen.

DISCUSSION

In this study, we identified two putative RLKs that are involved in shoot growth repression specifically under mannitol treatment but not any other osmotic stress-related treatment (Figure 4 and Figure S5). This suggests that mannitol not only generates a generic osmotic stress, but also acts as a specific signal that is transduced by EGM1 and EGM2 to alter transcription and growth. This hypothesis has been previously suggested in several non-mannitol-producing organisms transformed with either bacterial mannitol-1-phosphate dehydrogenase (*mt1D*) or celery (*Apium graveolens* L.) mannose-6-phosphate reductase (*M6PR*), in which enhanced resistance to salt, osmotic and/or drought stress were observed (Tarczynski *et al.*, 1993; Thomas *et al.*, 1995; Karakas *et al.*, 1997; Abebe *et al.*, 2003; Hu *et al.*, 2005). Interestingly, the amount of mannitol produced in those lines was too low to protect against stress through osmotic adjustment, suggesting that mannitol has other stress protective functions. In 2011, Chan *et al.* (2011) compared the transcriptomic response of *M6PR*-over-expressing *A. thaliana* lines with Col-0 under control and 100 mM NaCl stress conditions. As expected from the phenotypic analysis, Col-0 was transcriptionally more affected by salt than *M6PR*-over-expressing lines. Surprisingly, however, considering the absence of obvious macroscopic phenotype, the *M6PR* transgene altered the expression level of
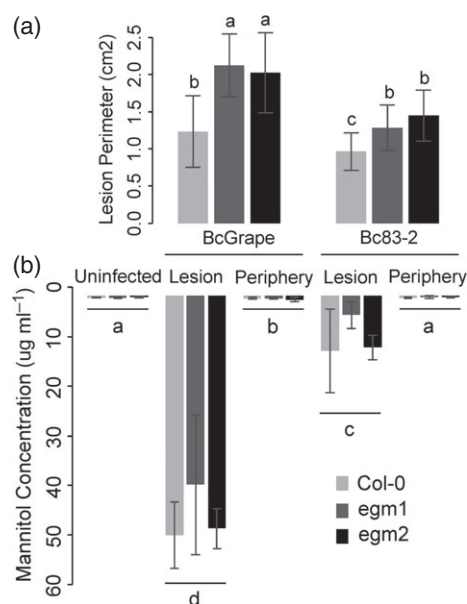
Figure 5. The role of EGM1 and EGM2 in the biotic stress response.
(a) Mean perimeter of necrotic lesions formed by *Botrytis cinerea* isolates BcGrape or Bc83-2 on wild-type, *egm1* and *egm2* mutant plants 72 h post-inoculation. Different letters indicate significantly different results based on a *post hoc* Tukey's honest significant difference test ($P < 0.05$).
(b) Mannitol concentrations observed within or at the periphery of necrotic lesions formed by *B. cinerea* isolates BcGrape or Bc83-2 on wild-type, *egm1* and *egm2* mutant plants 72 h post-inoculation. Different letters indicate significantly different results based on a *post hoc* Kruskal–Wallis test ($P < 0.05$).

2272 genes under control conditions, with enrichment of genes belonging to the GO categories 'response to stress', 'response to biotic and abiotic stimulus' and 'signal transduction'. Thus, *M6PR* expression and mannitol synthesis appeared to result in pre-adaptive changes facilitating responses to abiotic stress.

In addition to abiotic responses, the *M6PR* transgene appeared to have specific effects on genes involved in pathogen defense (Chan *et al.*, 2011). Skirycz *et al.* (2010) identified several biotic stress genes that were up-regulated in proliferating and expanding leaves under mannitol treatment. Global transcriptomic responses to mannitol in those tissues showed a significant overlap with publicly available microarrays analyzing biotic stress responses. This effect of mannitol on pathogen responsive genes has been interpreted as indicating indirect cross-talk between biotic and abiotic stress responses via antagonistic and synergistic relationships between abscisic acid and salicylic acid/jasmonic acid/ethylene and/or ROS generation and signaling (Fujita *et al.*, 2006). The up-regulation of these biotic stress-responsive genes has been interpreted as the result of activation of the ethylene signaling pathway (Skirycz *et al.*, 2010; Dubois *et al.*, 2013). Indeed, in expanding leaves, activation of the ethylene-responsive factors

ERF5 and ERF6 results in repression of gibberellic acid signaling, which ultimately limits cell-cycle progression and results in the activation of a gibberellic acid-independent response involving WRK33 (Dubois *et al.*, 2013). Interestingly, the *erf5 erf6* double mutant shows an enhanced shoot growth phenotype specifically under mannitol-induced stress (Dubois *et al.*, 2013). Several genes involved in ethylene signaling (including *ERF5*) were highlighted by our transcriptomic analysis (Table S2). These data strongly suggest that EGMs act upstream of the ERF5/ERF6 pathway; analysis of multiple mutants combining ERF factors and EGMs would provide interesting information in this regard.

In addition to the possibility of cross-talk between biotic and abiotic stress responses, an alternative hypothesis is that the regulation of pathogen responsive genes in response to mannitol may indicate a direct role of the mannitol/EGM system in plant defense. Given the identification of chitinases as genes that are specifically regulated by this system, we focused on the fungus *Botrytis cinerea*, which produces both chitin and mannitol. The *egm1* and *egm2* mutants were more sensitive than WT to the two *Botrytis* strains, and their sensitivity correlated with the amount of mannitol produced by the two strains within the plant lesion (Figure 5). Although this correlation between mannitol and pathogenicity may be fortuitous, it suggests that mannitol produced and secreted by pathogens during infection may be perceived more or less directly by the plant via an EGM1/EGM2-mediated pathway. In nature, plants probably encounter high concentrations of mannitol during infection with mannitol-producing pathogens (Voegele *et al.*, 2005) (Figure 5). In fungi, among other roles, mannitol is important for carbohydrate storage, as suggested by its relatively high concentration (Lewis and Smith, 1967; Solomon *et al.*, 2007). Although this role may not be essential for all fungi (Solomon *et al.*, 2007), it is particularly interesting for pathogens that infect plants that do not produce or metabolize mannitol, because the fungi may safely sequester carbon from the host in the form of mannitol (Voegele *et al.*, 2005; Dulermo *et al.*, 2009; Parker *et al.*, 2009). Several *in vitro* and *in vivo* studies have shown that mannitol probably plays a role in scavenging free radicals generated during stresses (Chaturvedi *et al.*, 1996b, 1997; Shen *et al.*, 1997; Voegele *et al.*, 2005). This role of mannitol may play a central role during host/pathogen interaction, because hosts often produce ROS species to counter pathogen attacks (Torres, 2010). As a result, it has been hypothesized that pathogens secrete mannitol to counteract host ROS production, although this may correspond to different strategies for biotrophic versus necrotrophic pathogens (Govrin and Levine, 2000). This hypothesis is supported by the increase in mannitol production and secretion by the pathogen [*Cladosporum fulvum* (Jennings *et al.*, 1998)] and the up-regulation of

mannitol synthesis enzymes during infection or treatment of the pathogen with plant leaf extract [*Alternaria alternata* (Velez *et al.*, 2008) and *Uromyces fabae* (Voegele *et al.*, 2005)]. In addition, some fungi mutated for mannitol biosynthesis genes, resulting in a strong reduction in mannitol content, have been shown to be less virulent than their WT [e.g. *A. alternata* (Velez *et al.*, 2008), *Cryptococus neoformans* (Chaturvedi *et al.*, 1996a) and *Alternaria brassicicola* (Calmes *et al.*, 2013)]. The role of mannitol in host/pathogen interactions is further supported by the fact that several plant mannitol dehydrogenases (MTDs), which convert mannitol to mannose, respond to biotic stress signals. For example, the celery *MTD* gene is up-regulated in response to salicylic acid (Williamson *et al.*, 1995; Zamski *et al.*, 2001; Cheng *et al.*, 2009). In tobacco (*Nicotiana tabacum*), which does not produce mannitol, an endogenous *MTD* gene whose activity is up-regulated by fungi and inducers of plant PR proteins (2,6-dichloroisonicotinic acid and H_2O_2) has been identified (Jennings *et al.*, 1998). Under treatment with salicylic acid, the product of the celery *MTD* gene over-expressed in tobacco is secreted in the apoplasm where fungi mannitol is also partly localized. Because this transgenic tobacco showed enhanced resistance to *A. alternata*, a mannitol-secreting pathogen, but not to *Cercospora nicotianae*, a non-mannitol-secreting fungus (Jennings *et al.*, 2002), it has been hypothesized that, in order to protect the plant's ROS-mediated defenses, plant MTDs are secreted in response to salicylic acid in the apoplast, where it converts the fungal-produced ROS-quencher mannitol into mannose (Cheng *et al.*, 2009).

Given the potentially important roles of mannitol for some fungi during plant infection (carbohydrate storage and ROS sequestration), it is possible that plants have developed specific mannitol-sensing pathways that contribute to response induction. Consistent with this hypothesis, we identified two SD1 RLKs that possibly contribute to pathogen defense via direct or indirect perception of mannitol. RLK receptors are known to be involved in a wide range of developmental processes such as hormone perception, reproduction, meristem regulation and cell/organ specification (Shiu and Bleecker, 2001a; Becraft, 2002; Gish and Clark, 2011), as well as the response to biotic and abiotic stresses, including kinases that are involved in transduction of osmotic stress signals as recently reviewed (Osakabe *et al.*, 2013). The most famous member of the SD1 sub-family is the *SRK* gene, which is the determinant of self-incompatibility specificity in Brassicaceae. In addition to potential developmental roles, this family has also been shown to be enriched in genes that are up-regulated by several biotic and abiotic stresses (Kilian *et al.*, 2007; Lehti-Shiu *et al.*, 2009). In addition, several homologs of *EGM1* and *EGM2* in *A. thaliana* [At1g11330 (Chae *et al.*, 2009); *At1 g11350/CBRLK1* (Kim *et al.*, 2009); *At1 g65790/ARK1* and *At4 g21380/ARK3* (Pastuglia *et al.*, 2002)] and

other species such as tobacco [*Nt-Sd-RLK* (Sanabria *et al.*, 2012) and *NgRLK1* (Kim *et al.*, 2010)] or rice [*Pi-d2* (Chen *et al.*, 2006)] are induced in response to salicylic acid, wounding and/or bacteria-generated stresses, and so are probably involved in biotic stress responses. Finally, this sub-family of receptors has contributed to expansion of the RLK/Pelle gene family in *A. thaliana*, an expansion that may be explained as a response to fast-evolving pathogens (Lehti-Shiu *et al.*, 2009).

In summary, these results suggest that EGM1 and EGM2 are involved in biotic responses that are probably mediated by mannitol. Future work is required to determine whether EGM1 and/or EGM2 directly interact with mannitol or whether they are downstream RLKs in the mannitol perception pathway, as well as testing whether mannitol or a related catabolite is the perceived chemical. Any sensing of mannitol associated with perception of other microbe-associated molecular patterns may contribute to the quantitative resistance of plants against mannitol-producing pathogens.

EXPERIMENTAL PROCEDURES

Plant material

All accessions and most of the mapping populations used in this study were obtained from the Versailles Arabidopsis Stock Center (http://publiclines.versailles.inra.fr/) or have been generated (Table S3). For the 'specific association genetics' approach, Cvi-like accessions were identified from a screen of approximately 500 accessions from the Versailles Arabidopsis Stock Center using two CAPS markers for polymorphisms 'e' and 'f' (Table S1) and analysis of the 1001 Genomes database for approximately 400 accessions (http://www.1001genomes.org/ and http://signal.salk.edu/atg1001/index.php). The region encompassing 500 bp of the *EGM1* promoter to the stop codon of *EGM2* (Table S1) and a 700 bp fragment around polymorphism 'a' (chromosome 1, position 3 790 103) were further sequenced in the seven Cvi-like accessions used for specific association genetics. All mutant lines were obtained from the Nottingham Arabidopsis Stock Centre (http://arabidopsis.info/) (Table S3). The primers used to genotype the lines are listed in Table S4.

Shoot growth estimations

Seeds were sterilized for 10 min in 70% EtOH with 0.1% Triton X-100, and rinsed for 10 min in 95% EtOH. They were stratified in 0.1% agar at 4°C in darkness for 3 days. Plants were sown on typical Arabidopsis growth medium: 2.5 mm KH_2PO_4, 2 mm $MgSO_4$, 2 mm $CaCl_2$, micro-elements (70 mm H_3BO_3, 14 mm $MnCl_2$, 0.5 mm $CuSO_4$, 0.2 mm Na_2MoO_4, 10 mm NaCl, 1 mm $ZnSO_4$, 0.01 mm $CoCl_2$), vitamins (27.7 mm *myo*-inositol, 4 mm niacin, 2.4 mm pyridoxine, 1.5 mm thiamin HCl, 0.21 mm biotin, 0.5 g L^{-1} calcium pantothenate), 0.8‰ Bromocresol purple, 0.07% MES, 0.005% ferric ammonium citrate, 5 mm KNO_3, 2.5 mm $Ca(NO_3)_2$, 1% sucrose and 1% PhytoBlend (Caisson Labs, http://www.caissonlabs.com), and on the same medium supplemented with the indicated concentration of mannitol (2.5–100 mm), KCl (110 mm), NaCl (110 mm), sorbitol (80–100 mm) or mannose (4 mm). Shoot area estimates were performed as described previously (Vlad *et al.*, 2010) by scanning the plates after flattening the

plants 12 days after sowing, and estimating the area of each seedling by image analysis.

For the specific association genetics approach, progeny testing of the segregation of EGM was tested in F_2 populations from diverse crosses under the same phenotyping conditions as above, using a genotypic marker linked to EGM (Tables S3 and S4). The segregation of EGM in a given cross was estimated from the contribution of the genotype effect on seedling shoot area on Man60 only (ANOVA: area = genotype × experiment × cross) and from the contribution of the genotype x medium component (ANOVA: area = genotype × medium × experiment × cross).

For the *in vivo* (soil-based) drought stress experiment, seeds were stratified in darkness at 4°C for 3 days. Fertiss plugs (filled with a mix of peatmoss soil and vermiculite, http://fertilnet.fr/en/) were saturated with nutritive solution and individually weighed. After 12 days on plugs at 80% of their saturated weight, 60 homogeneous plants per genotype were selected. On day 13, plugs were allowed to dry to 60% of their saturated weight. Thereafter, water content in the soil was checked every day by weighing each plug individually. From days 14–16, half of the plugs were not watered to allow them to dry to 30% of the saturated weight. The plugs were then maintained at 60% saturation (control conditions) and 30% saturation (mild drought stress conditions) for 8 more days. From days 14–25, photographs of the plants were taken. The total leaf area of each plant was estimated using ImageJ (Bouchabke *et al.*, 2008).

QTL mapping and fine-mapping

For QTL analysis, the seedling shoot area for each of the 164 RILs of the Cvi-0 × Col-0 RIL core set (RIL set 8RV from the Versailles Arabidopsis Stock Center; Simon *et al.*, 2008) was estimated from measurement of nine plants grown on control medium or medium supplemented with 60 mm mannitol. Multiple QTL Mapping and 2D scan analyses were performed on raw phenotypic data using the R/qtl package implemented in R (http://www.r-project.org). EGM R^2 was estimated using ANOVA at marker c1_04176. The significance threshold ($P < 0.05$) was estimated using a 1000-permutation test. EGM QTL segregation was confirmed in an HIF derived from RIL170. For fine-mapping, approximately 6000 descendants of the heterozygous HIF170 were screened for recombinants (rHIF). By analyzing the segregation of EGM in informative rHIFs, the candidate interval for the QTL was reduced to 10 kb. Advanced recombined HIFs (arHIFs) segregating solely for the 10 kb interval were obtained by fixing rHIF #40 and #59 for the Cvi allele and crossing these two fixed recombinants (Figure S1D).

Vector construction and plant transformations

All combinations of *EGM1* and *EGM2*, with or without the stop codon and 1 kb promoters (except p*EGM2*:*EGM2* and the 8 kb region from the promoter of *EGM1* to *EGM2*) were obtained by PCR amplification using Phusion high-fidelity Taq polymerase (Finnzymes, http://www.thermoscientificbio.com/finnzymes/) and the primer pairs containing recombination sequences listed in Table S4. Fragments were cloned into the pDONR207 entry vector (Invitrogen) via BP recombination according to the GATEWAY cloning procedure (Invitrogen, www.invitrogen.com), and subsequently transferred into various destination vectors (Table S4) via the LR recombination reaction. To obtain the pDONR207:p*EGM2*:*EGM2* construct, an *XhoI*/*Eco*0109I fragment (1.494 kb) from pDONR207:p*EGM2*:*EGM2* ExtraCellularDomain was ligated to an *XhoI*/*Eco*O109I fragment (5.863 kb) from pDONR207:*EGM2*(+stop) using T4 DNA ligase (Fermentas, http://www.thermoscientificbio.com/fermentas/) according to the manufacturer's instructions. To

obtain the pDONR207:p*EGM1*to*EGM2* construct, an *Alw*NI fragment from pDONR207:p*EGM1:EGM1* (4.773 kb) was ligated to an *Alw*NI fragment from pDONR207:p*EGM2:EGM2* (5.969 kb) using T4 DNA ligase (Fermentas) according to the manufacturer's instructions.

The artificial miRNA was designed using the WMD tool (http://wmd.weigelworld.org/) against a 21 nt sequence conserved between *EGM1* and *EGM2* but with less than 72% identity with other members of the SD1 sub-family of RLK. Amplification of the amiRNA was performed using pRS300 vector as recommended at http://wmd.weigelworld.org/, and cloned into pTOPO TA (Invitrogen). The amiRNA was then placed under the control of the constitutive CaMV 35S promoter by cloning the *Bam*HI/*Eco*RI insert from pTOPO:amiRNA into pHannibal (Wesley *et al.*, 2001) using T4 DNA ligase (Fermentas). Finally, the *Not*I-digested insert from pHannibal:amiRNA was cloned into the pGREENII0000 plant vector (Hellens *et al.*, 2000).

All constructs in plant destination vectors were transformed into electrocompetent C58C1 *Agrobacterium tumefaciens*, which was then used for agroinfiltration of the genotypes of interest (Table S4).

Quantitative PCR

Total RNA from 11-day-old seedlings was extracted using an RNeasy plant mini kit (Qiagen, http://www.qiagen.com/) and treated with RNase-free DNase I (Fermentas). Lack of DNA contamination was verified by PCR using at least 37.5 ng RNA, and first-strand cDNA was synthesized from 750 ng RNA using RevertAid H Minus reverse transcriptase (Fermentas) with oligo(dT)$_{18}$ in 20 μl reactions. The expression level of *EGM1* and *EGM2* was analyzed using TaqMan gene expression assays (*EGM1*, At02283577_g1; *EGM2*, At02283571_g1; protein phosphatase 2A subunit A3 [*PP2A*], At02284835_g1; glyceraldehyde-3-phosphate dehydrogenase [*GAPDH*], At02284919_g1) and TaqMan gene expression master mix (Applied Biosystems, https://bioinfo.appliedbiosystems.com/genome-database/gene-expression.html). Probe specificity was verified using specific DNA matrices. QPCR for genes other than *EGM1* and *EGM2* were performed using MESA GREEN qPCR MasterMix (Eurogentec, http://www.eurogentec.com) and the primer pairs indicated in Table S4. For the two techniques, 4 or 5 μl of 5 × diluted cDNA were used and reactions were performed on a Bio-Rad CFX96 real-time PCR detection machine according to the manufacturer's instructions. For each sample, we analyzed at least two technical and two biological replicates. The expression of each target was normalized against *PP2A* and *GAPDH* endogenous controls using the formula $2^{(C_t[Gi]-\text{mean}C_t[\text{endogenous control}])}$. For each biological replicate and target gene, the expression level of all samples was divided by that for the WT sample (arHIF[Col], Col-0 or WT) under control conditions, thereby setting the level of expression of the WT sample to 1 (except in Figure 3).

3′ RACE

Reverse transcription was performed on 500 ng of Col-0 total RNA using a polyT primer fused to a tail with sequence 5′-GACTCGAGTCGACATCTGTTTTTTTTTTTTTTTT-3′. PCR was performed on these cDNAs using a primer specific to the tail (ABO7: 5′-CAGATGTCGACTCGAGTC-3′) and a non-specific primer targeting the end of exon 7 of *At1 g11300* (20F: 5′-GCTGCTAACGATAGGCCAAG-3′). The amplified bands were purified on a gel, cloned into pTOPO using a TOPO TA kit (Invitrogen), and transformed into DH10β *Escherichia coli* cells. The PCR products obtained on five transformants using the ABO7 and 20F primers were sequenced using the 20F primer. Two of the transformants contained *At1 g11300* 3′ ends (similar) and two others contained *At1 g11305* 3′ ends (two different polyadenylation sites).

CATMA arrays

RNA from two pools per genotype of 12 DAS seedlings (days after sowing) grown on Man60 was extracted as described above, and total RNA was checked for quality by NanoChip analysis on an Agilent bioanalyzer (www.agilent.com), and quantified using Ribo-Green prior to microarray application. Transcript profiling was performed on CATMA version 5 microarrays at the Unité de Recherche en Génomique Végétale, France. Microarray hybridization, data analysis and the CATdb database have been described previously (Yang *et al.*, 2002; Gagnot *et al.*, 2008). The two genotypes compared on the array (arHIF[Col] and arHIF[Cvi]) have the same genomic background; therefore, even if there was any effect of the Col/Cvi sequence divergence on hybridization efficiency (which is unlikely with the CATMA probes), this would not result in differential gene expression. Microarray data were deposited at Gene Expression Omnibus (http://www.ncbi.nlm.nih.gov/geo/, accession number GSE36698) and at CATdb (http://urgv.evry.inra.fr/CATdb/; project RA09-01_QTLleafgrowth/ID 293).

For comparisons with the analysis by Skirycz *et al.* (2010), the transcriptomic response from expanding leaves of Col-0 treated with 25 mM mannitol was used. The overlap between the two sets comprising genes that were differentially expressed in the same direction in the two analyses was tested using the Genesect tool, a non-parametric randomization test available on the VIRTUAL PLANT 1.3 website (http://virtualplant.bio.nyu.edu/cgi-bin/vpweb/). The 20 250 TAIR version 10 gene models that are common between the CATMA version 5 arrays and the Affymetrix ATH1 arrays were used as the background list. Gene ontology analyses were performed using the Biomaps tool available on the VIRTUAL PLANT 1.3 website, which calculates *P* values of over-representation using Fisher's exact test with correction for the false discovery rate (Katari *et al.*, 2010).

GUS staining

GUS staining was performed on 12 DAS seedlings (T$_3$ generation) grown *in vitro* under control and Man60 conditions without fixation. Infiltration with X-Glu buffer (100 mM sodium phosphate buffer pH 7, 0.5 mM ferrocyanide, 0.5 mM ferricyanide, 8 mM X-Glu, diluted in dimethylsulfoxide) was performed under vacuum for 10 min. The samples were then kept at 37°C overnight, discolored the following day using 95% ethanol and the day after in 70% ethanol.

Phylogenetic analyses

Arabidopsis thaliana members of the SD1 subfamily of RLKs were retrieved from Lehti-Shiu *et al.* (2009), and as many SD1 *A. lyrata* homologs as possible were retrieved using the Protein homologs search available on the PHYTOZOME version 9.0 website (http://www.phytozome.net/). Protein sequences of 34 *A. thaliana* RLKs (32 SD1 members and two out-group RLKs from the SD2 sub-family) and 43 *A. lyrata* RLKs (including two close homologs of the *A. thaliana* out-group) were aligned using the program MUSCLE implemented in SEAVIEW version 4.2 (Gouy *et al.*, 2010), and the alignment obtained was manually improved in GENEDOC version 2.6.002 (http://www.nrbsc.org/gfx/genedoc/). The final alignment restricted to the kinase domain (amino acids 497–794 of EGM1) was used to align corresponding DNA coding sequences. To obtain the corresponding phylogeny, the best nucleotide substitution model fitting this alignment (GTR+I+G: GTR model with estimated proportion of invariable sites and Γ distribution) according

to the Akaike information criterion was determined using JMODELTEST version 2.1.1 (http://code.google.com/p/jmodeltest2/), and used to run a Bayesian inference analysis using MRBAYES version 3.2.1 (Huelsenbeck and Ronquist, 2001) with 1 000 000 generations and a burn-in of 5000 generations. The resulting phylogeny (including posterior probabilities as clade support values) was visualized in Treedyn (Chevenet *et al.*, 2006).

Botrytis assays

All *Botrytis cinerea* infections were performed as previously described using two previously characterized isolates (Rowe and Kliebenstein, 2008). All plants were grown in a randomized complete block design, and three leaves were taken from each plant, one for the control experiment and one for each of the two isolates, with a minimum of ten leaves per infection. Tissue was harvested from the uninfected part of each leaf, the lesion and the lesion boundary (periphery), and the mannitol content was analyzed using a GC-TOF-MS-based broad-spectrum platform (Fiehn *et al.*, 2008).

ACKNOWLEDGMENTS

SUPPORTING INFORMATION

Additional Supporting Information may be found in the online version of this article.

Figure S1. EGM QTL mapping and cloning.

Figure S2. T-DNA mutant analysis revealed that *EGM1* and *EGM2* are strong candidates for the EGM QTL.

Figure S3. Evolution of the SD1 sub-family.

Figure S4. Relative *EGM1* and *EGM2* expression levels in Col-0, Cvi-0 and Tou-1 accessions.

Figure S5. Additional data regarding the unlikely role of EGM1 and EGM2 in the abiotic stress response.

Figure S6. CATMA array results and additional quantitative PCR validation.

Figure S7. The role of EGM1 and EGM2 in the stress response.

Table S1. Polymorphisms observed in *EGM1* and *EGM2* in the accessions used for F_2 crosses.

Table S2. Differentially expressed genes between arHIF[Col] and arHIF[Cvi] under mannitol treatment.

Table S3. List of genetic materials used.

Table S4. List of primers and vectors used.

REFERENCES

Abebe, T., Guenzi, A.C., Martin, B. and Cushman, J.C. (2003) Tolerance of mannitol-accumulating transgenic wheat to water stress and salinity. *Plant Physiol.* **131**, 1748–1755.

Becraft, P.W. (2002) Receptor kinase signaling in plant development. *Annu. Rev. Cell Dev. Biol.* **18**, 163–192.

Bouchabke, O., Chang, F., Simon, M., Voisin, R., Pelletier, G. and Durand-Tardif, M. (2008) Natural variation in *Arabidopsis thaliana* as a tool for highlighting differential drought responses. *PLoS ONE*, **3**, e1705.

Calmes, B., Guillemette, T., Teyssier, L., Siegler, B., Pigne, S., Landreau, A., Iacomi, B., Lemoine, R., Richomme, P. and Simoneau, P. (2013) Role of mannitol metabolism in the pathogenicity of the necrotrophic fungus *Alternaria brassicicola*. *Front. Plant Sci.* **4**, 131.

Chae, L., Sudat, S., Dudoit, S., Zhu, T. and Luan, S. (2009) Diverse transcriptional programs associated with environmental stress and hormones in the Arabidopsis receptor-like kinase gene family. *Mol. Plant*, **2**, 84–107.

Chan, Z., Grumet, R. and Loescher, W. (2011) Global gene expression analysis of transgenic, mannitol-producing, and salt-tolerant *Arabidopsis thaliana* indicates widespread changes in abiotic and biotic stress-related genes. *J. Exp. Bot.* **62**, 4787–4803.

Chaturvedi, V., Flynn, T., Niehaus, W.G. and Wong, B. (1996a) Stress tolerance and pathogenic potential of a mannitol mutant of *Cryptococcus neoformans*. *Microbiology*, **142**, 937–943.

Chaturvedi, V., Wong, B. and Newman, S.L. (1996b) Oxidative killing of *Cryptococcus neoformans* by human neutrophils. Evidence that fungal mannitol protects by scavenging reactive oxygen intermediates. *J. Immunol.* **156**, 3836–3840.

Chaturvedi, V., Bartiss, A. and Wong, B. (1997) Expression of bacterial mtID in *Saccharomyces cerevisiae* results in mannitol synthesis and protects a glycerol-defective mutant from high-salt and oxidative stress. *J. Bacteriol.* **179**, 157–162.

Chen, X., Shang, J., Chen, D. et al. (2006) A B-lectin receptor kinase gene conferring rice blast resistance. *Plant J.* **46**, 794–804.

Cheng, F.Y., Zamski, E., Guo, W.W., Pharr, D.M. and Williamson, J.D. (2009) Salicylic acid stimulates secretion of the normally symplastic enzyme mannitol dehydrogenase: a possible defense against mannitol-secreting fungal pathogens. *Planta*, **230**, 1093–1103.

Chevenet, F., Brun, C., Banuls, A.L., Jacq, B. and Christen, R. (2006) Tree-Dyn: towards dynamic graphics and annotations for analyses of trees. *BMC Bioinformatics*, **7**, 439.

Dubois, M., Skirycz, A., Claeys, H. et al. (2013) ETHYLENE RESPONSE FACTOR6 acts as a central regulator of leaf growth under water-limiting conditions in Arabidopsis. *Plant Physiol.* **162**, 319–332.

Dulermo, T., Rascle, C., Chinnici, G., Gout, E., Bligny, R. and Cotton, P. (2009) Dynamic carbon transfer during pathogenesis of sunflower by the necrotrophic fungus *Botrytis cinerea*: from plant hexoses to mannitol. *New Phytol.* **183**, 1149–1162.

Fiehn, O., Wohlgemuth, G., Scholz, M., Kind, T., Lee do, Y., Lu, Y., Moon, S. and Nikolau, B. (2008) Quality control for plant metabolomics: reporting MSI-compliant studies. *Plant J.* **53**, 691–704.

Fujita, M., Fujita, Y., Noutoshi, Y., Takahashi, F., Narusaka, Y., Yamaguchi-Shinozaki, K. and Shinozaki, K. (2006) Crosstalk between abiotic and biotic stress responses: a current view from the points of convergence in the stress signaling networks. *Curr. Opin. Biotechnol.* **9**, 436–442.

Gagnot, S., Tamby, J.P., Martin-Magniette, M.L., Bitton, F., Taconnat, L., Balzergue, S., Aubourg, S., Renou, J.P., Lecharny, A. and Brunaud, V. (2008) CATdb: a public access to Arabidopsis transcriptome data from the URGV-CATMA platform. *Nucleic Acids Res.* **36**, 986–990.

Gish, L.A. and Clark, S.E. (2011) The RLK/Pelle family of kinases. *Plant J.* **66**, 117–127.

Gouy, M., Guindon, S. and Gascuel, O. (2010) SeaView version 4: a multi-platform graphical user interface for sequence alignment and phylogenetic tree building. *Mol. Biol. Evol.* **27**, 221–224.

Govrin, E.M. and Levine, A. (2000) The hypersensitive response facilitates plant infection by the necrotrophic pathogen *Botrytis cinerea*. *Curr. Biol.* **10**, 751–757.

Hellens, R.P., Edwards, E.A., Leyland, N.R., Bean, S. and Mullineaux, P.M. (2000) pGreen: a versatile and flexible binary Ti vector for *Agrobacterium*-mediated plant transformation. *Plant Mol. Biol.* **42**, 819–832.

Hu, L., Lu, H., Liu, Q., Chen, X. and Jiang, X. (2005) Overexpression of *mtID* gene in transgenic *Populus tomentosa* improves salt tolerance through accumulation of mannitol. *Tree Physiol.* **25**, 1273–1281.

Huelsenbeck, J.P. and Ronquist, F. (2001) MRBAYES: Bayesian inference of phylogenetic trees. *Bioinformatics*, **17**, 754–755.

Jennings, D.B., Ehrenshaft, M., Pharr, D.M. and Williamson, J.D. (1998) Roles for mannitol and mannitol dehydrogenase in active oxygen-mediated plant defense. *Proc. Natl Acad. Sci. USA*, **95**, 15129–15133.

Jennings, D.B., Daub, M.E., Pharr, D.M. and Williamson, J.D. (2002) Constitutive expression of a celery mannitol dehydrogenase in tobacco

enhances resistance to the mannitol-secreting fungal pathogen *Alternaria alternata*. *Plant J.* **32**, 41–49.

Karakas, B., Ozias-Akins, P., Stushnoff, C., Suefferheld, M. and Rieger, M. (1997) Salinity and drought tolerance of mannitol-accumulating transgenic tobacco. *Plant Cell Environ.* **20**, 609–616.

Katari, M.S., Nowicki, S.D., Aceituno, F.F. et al. (2010) VirtualPlant: a software platform to support systems biology research. *Plant Physiol.* **152**, 500–515.

Kilian, J., Whitehead, D., Horak, J., Wanke, D., Weinl, S., Batistic, O., D'Angelo, C., Bornberg-Bauer, E., Kudla, J. and Harter, K. (2007) The AtGenExpress global stress expression data set: protocols, evaluation and model data analysis of UV-B light, drought and cold stress responses. *Plant J.* **50**, 347–363.

Kim, H.S., Jung, M.S., Lee, S.M., Kim, K.E., Byun, H., Choi, M.S., Park, H.C., Cho, M.J. and Chung, W.S. (2009) An S-locus receptor-like kinase plays a role as a negative regulator in plant defense responses. *Biochem. Biophys. Res. Commun.* **381**, 424–428.

Kim, Y.T., Oh, J., Kim, K.H., Uhm, J.Y. and Lee, B.M. (2010) Isolation and characterization of NgRLK1, a receptor-like kinase of *Nicotiana glutinosa* that interacts with the elicitin of *Phytophthora capsici*. *Mol. Biol. Rep.* **37**, 717–727.

Klepek, Y.S., Geiger, D., Stadler, R., Klebl, F., Landouar-Arsivaud, L., Lemoine, R., Hedrich, R. and Sauer, N. (2005) Arabidopsis POLYOL TRANSPORTER5, a new member of the monosaccharide transporter-like superfamily, mediates H⁺-symport of numerous substrates, including myo-inositol, glycerol, and ribose. *Plant Cell*, **17**, 204–218.

Kreps, J.A., Wu, Y., Chang, H.S., Zhu, T., Wang, X. and Harper, J.F. (2002) Transcriptome changes for Arabidopsis in response to salt, osmotic, and cold stress. *Plant Physiol.* **130**, 2129–2141.

Lehti-Shiu, M.D., Zou, C., Hanada, K. and Shiu, S.H. (2009) Evolutionary history and stress regulation of plant receptor-like kinase/pelle genes. *Plant Physiol.* **150**, 12–26.

Lewis, D.H. and Smith, D.C. (1967) Sugar alcohols (polyols) in fungi and green plants: distribution, physiology and metabolism. *New Phytol.* **66**, 143–184.

Masle, J., Gilmore, S.R. and Farquhar, G.D. (2005) The ERECTA gene regulates plant transpiration efficiency in Arabidopsis. *Nature*, **436**, 866–870.

McMullen, B.A., Fujikawa, K. and Davie, E.W. (1991) Location of the disulfide bonds in human plasma prekallikrein: the presence of four novel apple domains in the amino-terminal portion of the molecule. *Biochemistry*, **30**, 2050–2056.

Osakabe, Y., Yamaguchi-Shinozaki, K., Shinozaki, K. and Tran, L.S. (2013) Sensing the environment: key roles of membrane-localized kinases in plant perception and response to abiotic stress. *J. Exp. Bot.* **64**, 445–458.

Parker, D., Beckmann, M., Zubair, H., Enot, D.P., Caracuel-Rios, Z., Overy, D.P., Snowdon, S., Talbot, N.J. and Draper, J. (2009) Metabolomic analysis reveals a common pattern of metabolic re-programming during invasion of three host plant species by *Magnaporthe grisea*. *Plant J.* **59**, 723–737.

Parre, E., Ghars, M.A., Leprince, A.S., Thiery, L., Lefebvre, D., Bordenave, M., Richard, L., Mazars, C., Abdelly, C. and Savoure, A. (2007) Calcium signaling via phospholipase C is essential for proline accumulation upon ionic but not nonionic hyperosmotic stresses in Arabidopsis. *Plant Physiol.* **144**, 503–512.

Pastuglia, M., Swarup, R., Rocher, A., Saindrenan, P., Roby, D., Dumas, C. and Cock, J.M. (2002) Comparison of the expression patterns of two small gene families of S gene family receptor kinase genes during the defence response in *Brassica oleracea* and *Arabidopsis thaliana*. *Gene*, **282**, 215–225.

Poormohammad Kiani, S., Trontin, C., Andreatta, M., Simon, M., Robert, T., Salt, D.E. and Loudet, O. (2012) Allelic heterogeneity and trade-off shape natural variation for response to soil micronutrient. *PLoS Genet.* **8**, e1002814.

Ramachandraiah, G. and Chandra, N.R. (2000) Sequence and structural determinants of mannose recognition. *Proteins*, **39**, 358–364.

Reinders, A., Panshyshyn, J.A. and Ward, J.M. (2005) Analysis of transport activity of Arabidopsis sugar alcohol permease homolog AtPLT5. *J. Biol. Chem.* **280**, 1594–1602.

Rowe, H.C. and Kliebenstein, D.J. (2008) Complex genetics control natural variation in *Arabidopsis thaliana* resistance to *Botrytis cinerea*. *Genetics*, **180**, 2237–2250.

Sanabria, N.M., van Heerden, H. and Dubery, I.A. (2012) Molecular characterisation and regulation of a *Nicotiana tabacum* S-domain receptor-like kinase gene induced during an early rapid response to lipopolysaccharides. *Gene*, **501**, 39–48.

Shen, B., Jensen, R.G. and Bohnert, H.J. (1997) Mannitol protects against oxidation by hydroxyl radicals. *Plant Physiol.* **115**, 527–532.

Shiu, S.H. and Bleecker, A.B. (2001a) Plant receptor-like kinase gene family: diversity, function, and signaling. *Sci. STKE*, **2001**, re22.

Shiu, S.H. and Bleecker, A.B. (2001b) Receptor-like kinases from Arabidopsis form a monophyletic gene family related to animal receptor kinases. *Proc. Natl Acad. Sci. USA*, **98**, 10763–10768.

Simon, M., Loudet, O., Durand, S., Bérard, A., Brunel, D., Sennesal, F.-X., Durand-Tardif, M., Pelletier, G. and Camilleri, C. (2008) QTL mapping in five new large RIL populations of *Arabidopsis thaliana* genotyped with consensus SNP markers. *Genetics*, **178**, 2253–2264.

Skirycz, A., De Bodt, S., Obata, T. et al. (2010) Developmental stage specificity and the role of mitochondrial metabolism in the response of Arabidopsis leaves to prolonged mild osmotic stress. *Plant Physiol.* **152**, 226–244.

Solomon, P.S., Waters, O.D. and Oliver, R.P. (2007) Decoding the mannitol enigma in filamentous fungi. *Trends Microbiol.* **15**, 257–262.

Stoop, J., Williamson, J. and Pharr, D.M. (1996) Mannitol metabolism in plants: a method for coping with stress. *Trends Plant Sci.* **1**, 139–144.

Tarczynski, M.C., Jensen, R.G. and Bohnert, H.J. (1993) Stress protection of transgenic tobacco by production of the osmolyte mannitol. *Science*, **259**, 508–510.

Thomas, J.C., Sepahi, M., Arendall, B. and Bohnert, H.J. (1995) Enhancement of seed germination in high salinity by engineering mannitol expression in *Arabidopsis thaliana*. *Plant Cell Environ.* **18**, 801–806.

Tordai, H., Banyai, L. and Patthy, L. (1999) The PAN module: the N-terminal domains of plasminogen and hepatocyte growth factor are homologous with the apple domains of the prekallikrein family and with a novel domain found in numerous nematode proteins. *FEBS Lett.* **461**, 63–67.

Torres, M.A. (2010) ROS in biotic interactions. *Physiol. Plant.* **138**, 414–429.

Trontin, C., Tisné, S., Bach, L. and Loudet, O. (2011) What does Arabidopsis natural variation teach us (and does not teach us) about adaptation in plants? *Curr. Opin. Plant Biol.* **14**, 225–231.

Velez, H., Glassbrook, N.J. and Daub, M.E. (2008) Mannitol biosynthesis is required for plant pathogenicity by *Alternaria alternata*. *FEMS Microbiol. Lett.* **285**, 122–129.

Verslues, P.E., Agarwal, M., Katiyar-Agarwal, S., Zhu, J. and Zhu, J.K. (2006) Methods and concepts in quantifying resistance to drought, salt and freezing, abiotic stresses that affect plant water status. *Plant J.* **45**, 523–539.

Vlad, D., Rappaport, F., Simon, M. and Loudet, O. (2010) Gene transposition causing natural variation for growth in *Arabidopsis thaliana*. *PLoS Genet.* **6**, e1000945.

Voegele, R.T., Hahn, M., Lohaus, G., Link, T., Heiser, I. and Mendgen, K. (2005) Possible roles for mannitol and mannitol dehydrogenase in the biotrophic plant pathogen *Uromyces fabae*. *Plant Physiol.* **137**, 190–198.

Wahl, V., Ponnu, J., Schlereth, A., Arrivault, S., Langenecker, T., Franke, A., Feil, R., Lunn, J.E., Stitt, M. and Schmid, M. (2013) Regulation of flowering by trehalose-6-phosphate signaling in *Arabidopsis thaliana*. *Science*, **339**, 704–707.

Wasano, N., Ohgushi, A. and Ohba, M. (2003) Mannose-specific lectin activity of parasporal proteins from a lepidoptera-specific *Bacillus thuringiensis* strain. *Curr. Microbiol.* **46**, 43–46.

Wesley, S.V., Helliwell, C.A., Smith, N.A. et al. (2001) Construct design for efficient, effective and high-throughput gene silencing in plants. *Plant J.* **27**, 581–590.

Williamson, J.D., Stoop, J.M., Massel, M.O., Conkling, M.A. and Pharr, D.M. (1995) Sequence analysis of a mannitol dehydrogenase cDNA from plants reveals a function for the pathogenesis-related protein ELI3. *Proc. Natl Acad. Sci. USA*, **92**, 7148–7152.

Yang, Y.H., Dudoit, S., Luu, P., Lin, D.M., Peng, V., Ngai, J. and Speed, T.P. (2002) Normalization for cDNA microarray data: a robust composite method addressing single and multiple slide systematic variation. *Nucleic Acids Res.* **30**, e15.

Zamski, E., Guo, W.W., Yamamoto, Y.T., Pharr, D.M. and Williamson, J.D. (2001) Analysis of celery (*Apium graveolens*) mannitol dehydrogenase (Mtd) promoter regulation in Arabidopsis suggests roles for MTD in key environmental and metabolic responses. *Plant Mol. Biol.* **47**, 621–631.